Normal-Mode Splitting in a Weakly Coupled Optomechanical System

Massimiliano Rossi,[1,2,*] Nenad Kralj,[2] Stefano Zippilli,[2,3] Riccardo Natali,[2,3] Antonio Borrielli,[4] Gregory Pandraud,[5] Enrico Serra,[5,6] Giovanni Di Giuseppe,[2,3,†] and David Vitali[2,3,7,‡]

[1]*School of Higher Studies "C. Urbani", University of Camerino, 62032 Camerino, Macerata, Italy*
[2]*School of Science and Technology, Physics Division, University of Camerino, 62032 Camerino, Macerata, Italy*
[3]*INFN, Sezione di Perugia, 06123 Perugia, Italy*
[4]*Institute of Materials for Electronics and Magnetism, Nanoscience-Trento-FBK Division, 38123 Povo, Trento, Italy*
[5]*Delft University of Technology, Else Kooi Laboratory, 2628 Delft, The Netherlands*
[6]*Istituto Nazionale di Fisica Nucleare, TIFPA, 38123 Povo, Trento, Italy*
[7]*CNR-INO, L.go Enrico Fermi 6, I-50125 Firenze, Italy*

(Received 19 August 2017; published 12 February 2018)

Normal-mode splitting is the most evident signature of strong coupling between two interacting subsystems. It occurs when two subsystems exchange energy between themselves faster than they dissipate it to the environment. Here we experimentally show that a weakly coupled optomechanical system at room temperature can manifest normal-mode splitting when the pump field fluctuations are antisquashed by a phase-sensitive feedback loop operating close to its instability threshold. Under these conditions the optical cavity exhibits an effectively reduced decay rate, so that the system is effectively promoted to the strong coupling regime.

DOI: 10.1103/PhysRevLett.120.073601

Normal-mode splitting is the hallmark of strongly coupled systems. In this regime two interacting systems exchange excitations faster than they are dissipated, and form collective normal modes the hybridized excitations of which are superpositions of the constituent systems' excitations [1,2]. This regime is necessary for the observation of coherent quantum dynamics of the interacting systems and is a central achievement in research aimed at the control and manipulation of quantum systems [3]. In cavity opto- or electromechanics, where electromagnetic fields and mechanical resonators interact via radiation pressure, normal-mode splitting and strong coupling have already been obtained, using sufficiently strong power of the input driving electromagnetic field [4], or working at cryogenic temperatures with relatively large single-photon coupling [5,6].

In this Letter we report on the oxymoron of observing normal-mode splitting in a weakly coupled system. Specifically, we have designed and implemented a feedback system [7,8] which permits the formation of hybridized normal modes also at room temperature and in a relatively modest device, in terms of single-photon optomechanical interaction strength (as compared to the devices used in Refs. [4–6]). Our system is basically weakly coupled at the driving power that we can use (limited by the onset of optomechanical bistability at stronger power), and the emergence of hybridized optomechanical modes is observed when the light amplitude at the cavity output is detected and used to modulate the amplitude of the input field driving the cavity itself. The feedback works in the antisquashing regime, close to the feedback instability, where light fluctuations are enhanced over a narrow frequency range around the cavity resonance. In this regime the system behaves effectively as an equivalent optomechanical system with reduced cavity linewidth. This allows coherent energy oscillations between light and vibrational degrees of freedom when, for example, a coherent light pulse is injected into the cavity mode, similar to what has been discussed in Ref. [6].

Light (anti-) squashing [9–11] refers to an in-loop (enhancement) reduction of light fluctuations within a (positive) negative feedback loop. Even if the subshot noise features of in-loop light disappear out of the loop, so that squashing is different from real squeezing [9], useful applications of in-loop light have been proposed [10,11] and realized [7,8]. In this context, the results presented here demonstrate the potentiality of the in-loop cavity as a novel powerful tool for manipulating mechanical systems. It can be useful in situations that require a reduced cavity decay or when, due to technical limitations, increasing the pump power is not a viable option, e.g., in the case of optomechanical bistability (as in our system) or large absorption (which may lead to detrimental thermorefractive effects, in turn detuning the cavity mode [12]). Our results apply directly to the high-temperature classical regime. However, as already discussed in the case of ground state cooling [7], this technique can also be successfully applied to the control of mechanical resonators at the quantum level.

Our system, described in more detail in Refs. [7,8,13], consists of a double-sided, symmetric, optical Fabry-Pérot

cavity and a low-absorption [13] circular SiN membrane in a membrane-in-the-middle setup [14]. We focus on the fundamental mechanical mode, with resonance frequency $\omega_m = 2\pi \times 343.13$ kHz and a decay rate $\gamma_m = 2\pi \times 1.18$ Hz [7,8]. The cavity has an empty-cavity finesse of $\mathcal{F}_0 = 42\,000$, corresponding to an amplitude decay rate $\kappa = 2\pi \times 20$ kHz [7,8]. Experimentally, these values are determined by placing the membrane at a node (or an antinode) of the cavity standing wave, since the finesse is generally diminished by the membrane optical absorption and surface roughness, and is a periodic function of its position [13,15].

The experimental setup is shown in Fig. 1. Two laser beams are utilized. The probe beam is used both to lock the laser frequency to the cavity resonance and to monitor the cavity phase fluctuations via balanced homodyne detection. The cooling (pump) beam, detuned by a frequency Δ from the cavity resonance by means of two acousto-optic modulators (shown schematically as AOM in Fig. 1), drives the optical cavity and provides the optomechanical interaction. This field is not a coherent, free field, but is subjected to feedback; i.e., it is an in-loop field. After being filtered by the cavity, the amplitude quadrature of the transmitted field is directly detected with a single photodiode. The resulting photocurrent is amplified, filtered, and fed back to the AOM driver in order to modulate the amplitude of the input field, thus closing the loop. The full characterization of the feedback response function is reported in Refs. [7,8], where we have already demonstrated that this kind of feedback can be employed to enhance the efficiency of optomechanical sideband cooling. In particular, we have showed how the in-loop spectra change when the feedback goes from positive to negative.

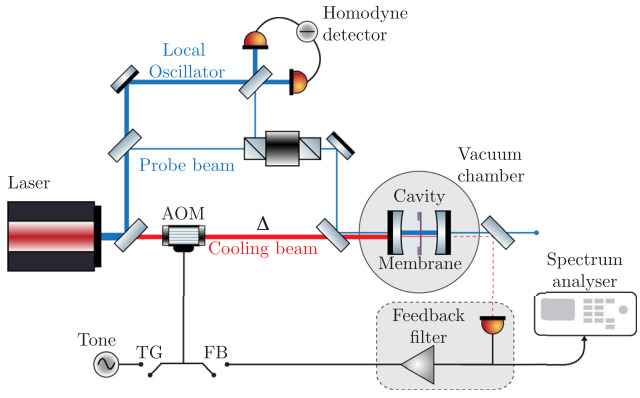

FIG. 1. A 1064 nm laser generates two beams. The probe beam, indicated by blue lines, is used to lock the laser frequency to the cavity resonance. Its phase, in which the membrane mechanical motion is encoded, is monitored with a homodyne scheme. The cooling beam, represented by red lines, provides the optomechanical interaction and is enclosed within a feedback loop. After being transmitted by the cavity, its amplitude is detected and the resulting signal is electronically processed and used to modulate the amplitude of the input field. In this way both the noise properties of light and the cavity susceptibility are modified.

Enclosing the optical cavity within the loop [7–11,16] effectively modifies its susceptibility for the in-loop optical field, such that (see also Ref. [17])

$$\tilde{\chi}_c^{\mathrm{eff}}(\omega) = \frac{\tilde{\chi}_c(\omega)}{1 - \tilde{\chi}_{\mathrm{fb}}(\omega)[\tilde{\chi}_c(\omega)e^{-i\theta_\Delta} + \tilde{\chi}_c^*(-\omega)e^{i\theta_\Delta}]}, \quad (1)$$

where $\tilde{\chi}_c(\omega) = [\kappa + i(\omega - \Delta)]^{-1}$ is the cavity susceptibility, $\tilde{\chi}_{\mathrm{fb}}(\omega) = \eta\sqrt{2\kappa_0}2\kappa'\sqrt{n_s}\tilde{g}_{\mathrm{fb}}(\omega)$, with η the detection efficiency, κ_0 and κ' the input and output cavity decay rate, respectively, n_s the mean intracavity photon number, and $\tilde{g}_{\mathrm{fb}}(\omega)$ the feedback control function $[\tilde{g}_{\mathrm{fb}}^*(-\omega) = \tilde{g}_{\mathrm{fb}}(\omega)]$. Furthermore, the dimensionless displacement of the mechanical oscillator measured by the out-of-loop probe beam, $\delta\tilde{q} = \tilde{\chi}_m^{o,\mathrm{eff}}(\omega)[\tilde{\xi}(\omega) + \tilde{\mathcal{N}}^{\mathrm{eff}}(\omega)]$ [17], is the sum of a term proportional to thermal noise, described by the zero mean stochastic noise operator $\tilde{\xi}(\omega)$, and a term due to the interaction with the cavity, proportional to radiation pressure noise, reshaped by the effective cavity susceptibility according to the relation $\tilde{\mathcal{N}}^{\mathrm{eff}}(\omega) = G\{\tilde{\chi}_c^{\mathrm{eff}}(\omega)\tilde{n} + [\tilde{\chi}_c^{\mathrm{eff}}(\omega)]^*\tilde{n}^\dagger\}$, with $\tilde{n}$ the radiation pressure noise operator [17] and $G = g_0\sqrt{2n_s}$ the (many-photon) optomechanical coupling strength [2,24], where g_0 is the single-photon optomechanical coupling. Finally, in the expression for the mechanical displacement, the factor $\tilde{\chi}_m^{o,\mathrm{eff}}(\omega)$ is the modified mechanical susceptibility that is dressed by the effective self-energy $\Sigma^{\mathrm{eff}}(\omega) = -iG^2\{\tilde{\chi}_c^{\mathrm{eff}}(\omega) - [\tilde{\chi}_c^{\mathrm{eff}}(-\omega)]^*\}$ according to

$$[\tilde{\chi}_m^{o,\mathrm{eff}}(\omega)]^{-1} = [\tilde{\chi}_m(\omega)]^{-1} + \Sigma^{\mathrm{eff}}(\omega), \quad (2)$$

where the bare susceptibility is $[\tilde{\chi}_m(\omega)]^{-1} = (\omega_m^2 - \omega^2 - i\omega\gamma_m)/\omega_m$.

In the resolved sideband limit, $\omega_m \gg \kappa$, and for $\Delta \sim \omega_m$ in order to cool the resonator, the effective cavity susceptibility for frequencies close to the cavity resonance $\omega \sim \Delta$ can be approximated as $\tilde{\chi}_c^{\mathrm{eff}}(\omega) \sim [\kappa_{\mathrm{eff}} + i(\Delta_{\mathrm{eff}} - \omega)]^{-1}$, where $\kappa_{\mathrm{eff}} = \kappa + \mathrm{Im}[\tilde{\chi}_{\mathrm{fb}}(\Delta)]$ and $\Delta_{\mathrm{eff}} = \Delta - \mathrm{Re}[\tilde{\chi}_{\mathrm{fb}}(\Delta)]$. These relations allow us to significantly simplify the expressions reported above and interpret the system dynamics in terms of that of a standard optomechanical system with a modified cavity. In particular, in the positive feedback regime (corresponding to light antisquashing) the in-loop optical mode experiences an effectively reduced decay rate, which tends to zero as the feedback gain is increased and approaches the feedback instability [7,8]. This in turn amounts to an increased optomechanical cooperativity $C_{\mathrm{eff}} = 2G^2/\kappa_{\mathrm{eff}}\gamma_m$. In Refs. [7,8] we have correspondingly shown that this effect can be employed to augment the mechanical damping rate Γ_{eff} and hence to improve sideband cooling of mechanical motion. Here we

demonstrate that in-loop optical cavities represent a new, powerful tool for reaching the strong coupling regime, owing to an effective reduction of the cavity linewidth $\kappa_{\rm eff}$.

Normal-mode splitting is a clear signature of strong coupling, being that it is only observable above the threshold $G \gtrsim \kappa_{\rm eff}$ [2,4] (in typical optomechanical systems the other condition $G > \gamma_m$ is easily satisfied). Since both normal modes are combinations of light and mechanical modes, they are both visible in the detectable mechanical displacement spectrum as distinct peaks at frequencies $\omega_\pm$, separated by $\omega_+ - \omega_- \simeq \sqrt{2}G$ when $\Delta_{\rm eff} = \omega_m$. The two peaks are distinguishable if the corresponding linewidths, which are of the order of $\kappa_{\rm eff}$, are smaller than G. In particular, strong coupling manifests itself as avoided crossing for the values of the normal frequencies $\omega_\pm$ when the cavity detuning is varied. This is apparent from Fig. 2, showing the spectra of the displacement fluctuations of the mechanical mode interacting with the in-loop optical mode, recorded via homodyne detection of the probe beam. In Fig. 2(a) a color plot is used to show these spectra as a function of frequency and normalized detuning, acquired with the maximum attainable feedback gain, and panel (b) is the theoretical expectation. The parameters used for the simulation, determined independently, are the decay rate $\kappa = 2\pi \times 22$ kHz, the single-photon optomechanical coupling estimated to be $g_0 = 2\pi \times 1.8$ Hz at this membrane position, and the input cooling power $P = 10$ μW. These parameters correspond to $G \sim 2\pi \times 3836$ Hz, which is larger than γ_m, but lower than κ, implying that the optomechanical system is initially far from the strong coupling regime. The feedback is then set to operate in the antisquashing regime, with such a value of gain that the

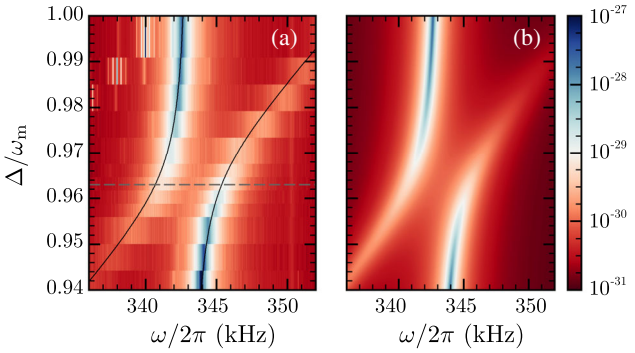

FIG. 2. Normal mode splitting. (a) Measured and (b) theoretically predicted splitting of the fundamental mechanical mode in the strong coupling regime as a function of detuning, with the two normal modes exhibiting avoided crossing. The dashed gray line indicates the optimal value of the detuning for sideband cooling with feedback. The values of the color scale are in m^2/Hz and correspond to the displacement spectral noise evaluated as $S_{xx}(\omega) = x_0^2 S_{qq}(\omega)$ with $x_0 = \sqrt{\hbar/2m\omega_m}$ the zero point motion factor, and $S_{qq}(\omega)$ the power spectrum of the dimensionless displacement operator δq [17].

threshold $G \sim \kappa_{\rm eff}$ is surpassed and normal mode splitting becomes visible.

Let us now analyze these spectra in more detail. In the resolved sideband limit, the symmetrized displacement noise spectrum can be expressed as [17]

$$S_{qq}(\omega) \simeq |\tilde{\chi}_m^{\rm o,eff}(\omega)|^2 [S_{\rm th} + S_{\rm rp}^{\rm eff}(\omega) + S_{\rm fb}(\omega)], \qquad (3)$$

where the first two terms account for the standard spectrum (with no feedback) for an optomechanical system, but with cavity decay rate $\kappa_{\rm eff}$, and the last term can be interpreted as additional noise due to the feedback and is given by [17]

$$S_{\rm fb}(\omega) \sim G^2 \mathcal{Z}^{\Delta} [|\tilde{\chi}_c^{\rm eff}(\omega)|^2 + |[\tilde{\chi}_c^{\rm eff}(-\omega)]|^2], \qquad (4)$$

which has the same form of the radiation pressure term, except for the factor $\mathcal{Z}^{\Delta} = [(\Delta - \Delta_{\rm eff})^2 + (\kappa_{\rm eff} - \kappa)^2]/2\eta\kappa'$ replacing $\kappa_{\rm eff}$. Figure 3 shows the spectrum of the fundamental mechanical mode excited by thermal fluctuations at 300 K (blue trace), with an optomechanical contribution due to the quasiresonant probe beam with 15 μW of power, which slightly cools down the mechanical mode, increasing the damping rate by a factor of ~2.8, due to an estimated probe detuning of around $2\pi \times 300$ Hz. The red trace demonstrates the standard (no feedback) sideband–cooling due to the cooling beam with a detuning set to $\Delta = 2\pi \times 330$ kHz, and the other optomechanical parameters set as for the data in Fig. 2, such that the strong coupling regime is initially not reached. Finally, the green

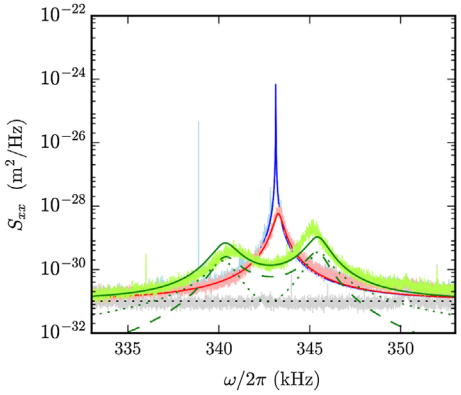

FIG. 3. Displacement spectral noise $S_{xx}(\omega) = x_0^2 S_{qq}(\omega)$ with $x_0 = \sqrt{\hbar/2m\omega_m}$ and offset by the shot-noise gray trace, of the (0,1) membrane mode at room temperature (blue trace), and sideband cooled (red trace) with a pump of $P = 10$ μW detuned by $\Delta = 330$ kHz. Increasing the gain with the feedback operating in the antisquashing regime effectively reduces the cavity linewidth, allowing us to enter the strong coupling regime, as seen from the appearance of two hybrid modes (green trace). The green, solid line represents the theoretical expectation according to Eq. (3), and is the sum of the comparable thermal and feedback terms shown as the dotted and dashed line, respectively, while the radiation pressure contribution is negligible. The narrow feature at ~339 kHz is a calibration tone.

trace corresponds to the cross section of Fig. 2(a) indicated by the gray dashed line. In this particular case we estimate, from the experimental data and the simulation, the effective parameters $\kappa_{\rm eff} \sim 2\pi \times 1210\,{\rm Hz}$ and $\Delta_{\rm eff} \sim 2\pi \times 342.65\,{\rm kHz}$. Since $\mathcal{Z}^{\Delta} \gg \kappa_{\rm eff}$ in the range of parameters relevant to our experiment, the feedback noise, differently from the radiation pressure term, provides a non-negligible contribution to the overall spectrum with respect to the thermal one, as indicated by the dashed and dotted lines.

The results we have presented are obtained in a condition in which the pump field efficiently cools the mechanical resonator [7,8]. In general, when an optomechanical system enters the strong coupling regime, the efficiency of sideband cooling decreases. Hereafter, we report on the similar effect that we observe as we increase the feedback gain towards instability, while keeping the other parameters fixed, as shown in Fig. 4. Panel (a) presents a plot of the mechanical displacement spectra as a function of frequency and feedback gain $\mathcal{G}_{\rm fb} = -{\rm Im}[\tilde{\chi}_{\rm fb}(\Delta)]/\kappa$, normalized in such a way that $\mathcal{G}_{\rm fb} = 1$ when $\kappa_{\rm eff} = 0$, i.e., at the feedback stability threshold. In panel (b) we report the corresponding and consistent results simulated using the theoretical model with the previously listed parameters for the membrane mode, $P = 26\ \mu{\rm W}$ and $\Delta = 2\pi \times 334.9$ kHz for the optical pump, $\kappa = 2\pi \times 21$ kHz and $g_0 = 2\pi \times 0.6$ Hz. Finally, panel (c) shows that at low gain values the cooling efficiency increases with the feedback gain. As explained previously, this effect can be understood as a result of the increment in the optomechanical cooperativity due to the effectively reduced in-loop cavity decay rate. We further note that, as expected, the enhanced cooperativity does not imply an improvement of optical cooling all the way towards the instability point. Rather, the cooling works well in the weak-coupling limit, i.e., when the cavity response time $\kappa_{\rm eff}^{-1}$ is shorter than the decay time of the oscillator modified by the optomechanical interaction $\Gamma_{\rm eff}^{-1}$, so as to allow mechanical thermal energy to be transferred into the cavity mode and leak out [24]. Conversely, around the threshold $\kappa_{\rm eff} \sim G$ the overall mechanical damping rate is of the order of the cavity linewidth, $\Gamma_{\rm eff} \sim \kappa_{\rm eff}$, and as the gain is increased further, $\Gamma_{\rm eff}$ grows, while $\kappa_{\rm eff}$ gets smaller, such that the cooling efficiency decreases. In particular, for high temperature, in the resolved sideband limit, $\kappa_{\rm eff} \ll \Delta_{\rm eff} \sim \omega_m$, small optomechanical coupling $G \ll \omega_m$, and a small mechanical decay rate $\gamma_m \ll (\Gamma_{\rm eff}, \kappa_{\rm eff})$, the steady state average number of mechanical excitations n_m can be evaluated in terms of the integral of the spectrum $S_{qq}(\omega)$ [24], and it is given by [17]

$$n_m \sim n_m^{\rm th,eff} \frac{\gamma_m}{\Gamma_{\rm eff}} \left(1 + \frac{\Gamma_{\rm eff}}{2\kappa_{\rm eff}}\right), \tag{5}$$

which is equal to the result for a standard optomechanical system (with no feedback), but with cavity decay rate $\kappa_{\rm eff}$, and in a higher temperature reservoir $n_m^{\rm th,eff} \sim n_m^{\rm th} + n_m^{\rm eff}$, with

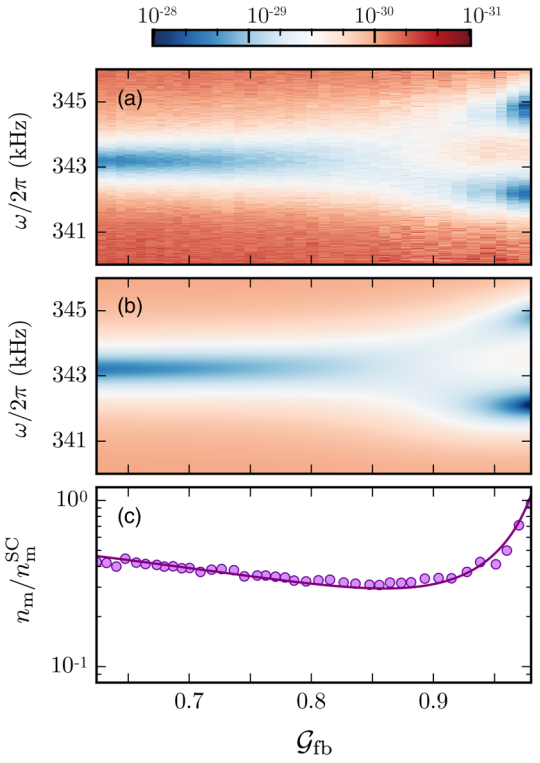

FIG. 4. Transition between the weak- and strong coupling regime. (a) Power spectra of mechanical displacement fluctuations varying the feedback gain $\mathcal{G}_{\rm fb}$, and (b) the corresponding simulation evaluated as $S_{xx}(\omega) = x_0^2 S_{qq}(\omega)$ with $x_0 = \sqrt{\hbar/2m\omega_m}$. The color scale is shown at the top in m^2/Hz. At low gain the mechanical motion is described by a single mode, the dynamics of which is modified by the in-loop optomechanical interaction. At high gain, instead, the spectrum becomes double-peaked: the strong interaction produces hybridized optomechanical modes and the mechanical motion is a superposition of these two normal modes. The difference in frequency between the two peaks in the spectrum with maximum gain corresponds to $G = 2\pi \times 1.87$ kHz. The parameters for this measurement (P, Δ, κ and g_0) yield $G = 2\pi \times 1.96$ kHz, in good agreement with the experimental estimation. (c) The ratio of the effective phonon number with and without feedback. The circles are obtained by numerical integration of the measured spectra, while the solid line corresponds to Eq. (5), evaluated using the measured parameters, which is valid both in the weak- and in the strong coupling regime. The feedback scheme enhances the cooling rate with respect to standard sideband cooling by a factor of 5 dB.

$$n_m^{\rm eff} \sim \frac{\mathcal{Z}^{\Delta}\Gamma_{\rm eff}}{\gamma_m(2\kappa_{\rm eff} + \Gamma_{\rm eff})}. \tag{6}$$

The validity of this result is demonstrated in Fig. 4(c) where we report the effective phonon number of the mechanical mode, normalized with respect to the occupancy obtained by standard sideband cooling without feedback, $n_m^{\rm SC}$. In particular, the solid line, which is in very good agreement with the data (dots), represents the expected average phonon number defined in Eq. (5). The optimal cooling

gain is $\mathcal{G}_{\mathrm{fb}} \approx 0.9$, and beyond this value the spectrum becomes double peaked [Figs. 4(a) and 4(b)], indicating that the system enters the strong coupling regime.

To conclude, we emphasize that, as demonstrated by our results, feedback-controlled light represents a promising approach to the control of the optomechanical dynamics which offers the possibility to tune the effective cavity linewidth at will. In particular, herein we have shown that this allows us to access the regime of strong coupling, characterized by the emergence of hybridized normal modes, even when the optomechanical interaction is small as compared to the natural dissipation rates, so that the original system is in fact weakly coupled. In our experiment, using the optimal parameters of Fig. 2, the effective cavity decay rate is reduced by a factor 20, and the system is promoted to the strong coupling regime with an estimated cooperativity parameter of $C_{\mathrm{eff}} \simeq 2 \times 10^4$. We further note that the ability to effectively reduce the cavity linewidth may ease tasks such as transduction, storage, and retrieval of signals and energy [25–27] with low frequency massive resonators. Finally, this technique could also be exploited to improve certain protocols for the preparation of nonclassical mechanical states [28], which are more efficient at low cavity decay rate, or to enhance the efficiency of mechanical heat engines that work in the strong coupling regime [29] or which make use of correlated reservoirs [30].

We acknowledge the support of the European Union's Horizon 2020 research and innovation program under Grant agreement No. 732894 (FET Proactive HOT).

*Present address: Niels Bohr Institute, University of Copenhagen, Blegdamsvej 17, 2100 Copenhagen, Denmark.
†gianni.digiuseppe@unicam.it
‡david.vitali@unicam.it

[1] H. J. Kimble, Phys. Scr. **T76**, 127 (1998).
[2] J. M. Dobrindt, I. Wilson-Rae, and T. J. Kippenberg, Phys. Rev. Lett. **101**, 263602 (2008).
[3] R. J. Thompson, G. Rempe, and H. J. Kimble, Phys. Rev. Lett. **68**, 1132 (1992); C. Weisbuch, M. Nishioka, A. Ishikawa, and Y. Arakawa, Phys. Rev. Lett. **69**, 3314 (1992); A. Wallraff, D. I. Schuster, A. Blais, L. Frunzio, R.-S. Huang, J. Majer, S. Kumar, S. M. Girvin, and R. J. Schoelkopf, Nature (London) **431**, 162 (2004); J. P. Reithmaier, G. Sęk, A. Löffler, C. Hofmann, S. Kuhn, S. Reitzenstein, L. V. Keldysh, V. D. Kulakovskii, T. L. Reinecke, and A. Forchel, Nature (London) **432**, 197 (2004); T. Yoshie, A. Scherer, J. Hendrickson, G. Khitrova, H. M. Gibbs, G. Rupper, C. Ell, O. B. Shchekin, and D. G. Deppe, Nature (London) **432**, 200 (2004); K. Hennessy, A. Badolato, M. Winger, D. Gerace, M. Atatüre, S. Gulde, S. Fält, E. L. Hu, and A. Imamoğlu, Nature (London) **445**, 896 (2007).
[4] S. Gröblacher, K. Hammerer, M. R. Vanner, and M. Aspelmeyer Nature (London) **460**, 724 (2009).
[5] J. D. Teufel, D. Li, M. S. Allman, K. Cicak, A. J. Sirois, J. D. Whittaker, and R. W. Simmonds, Nature (London) **471**, 204 (2011).
[6] E. Verhagen, S. Deléglise, S. Weis, A. Schliesser, and T. J. Kippenberg, Nature (London) **482**, 63 (2012).
[7] M. Rossi, N. Kralj, S. Zippilli, R. Natali, A. Borrielli, G. Pandraud, E. Serra, G. Di Giuseppe, and D. Vitali, Phys. Rev. Lett. **119**, 123603 (2017).
[8] N. Kralj *et al.*, Quantum Sci. Technol. **2**, 034014 (2017).
[9] J. H. Shapiro, G. Saplakoglu, S.-T. Ho, P. Kumar, B. E. A. Saleh, and M. C. Teich, J. Opt. Soc. Am. B **4**, 1604 (1987).
[10] H. M. Wiseman, Phys. Rev. Lett. **81**, 3840 (1998).
[11] H. M. Wiseman, J. Opt. B **1**, 459 (1999).
[12] D. Parrain, C. Baker, G. Wang, B. Guha, E. G. Santos, A. Lemaitre, P. Senellart, G. Leo, S. Ducci, and I. Favero, Opt. Express **23**, 19656 (2015).
[13] E. Serra *et al.*, AIP Adv. **6**, 065004 (2016).
[14] J. D. Thompson, B. M. Zwickl, A. M. Jayich, F. Marquardt, S. M. Girvin, and J. G. E. Harris, Nature (London) **452**, 72 (2008).
[15] C. Biancofiore, M. Karuza, M. Galassi, R. Natali, P. Tombesi, G. Di Giuseppe, and D. Vitali, Phys. Rev. A **84**, 033814 (2011).
[16] M. S. Taubman, H. Wiseman, D. E. McClelland, and H.-A. Bachor, J. Opt. Soc. Am. B **12**, 1792 (1995).
[17] See Supplemental Material at http://link.aps.org/supplemental/10.1103/PhysRevLett.120.073601 for additional details on the theoretical model and for additional results about optomechanical induced transparency in this system, which includes Refs. [7, 18–24].
[18] V. Giovannetti and D. Vitali, Phys. Rev. A **63**, 023812 (2001).
[19] S. Weis, R. Riviere, S. Deleglise, E. Gavartin, O. Arcizet, A. Schliesser, and T. J. Kippenberg, Science **330**, 1520 (2010).
[20] A. H. Safavi-Naeini, T. P. Mayer Alegre, J. Chan, M. Eichenfield, M. Winger, Q. Lin, J. T. Hill, D. E. Chang, and O. Painter, Nature (London) **472**, 69 (2011).
[21] M. Karuza, C. Biancofiore, M. Bawaj, C. Molinelli, M. Galassi, R. Natali, P. Tombesi, G. Di Giuseppe, and D. Vitali, Phys. Rev. A **88**, 013804 (2013).
[22] U. Fano, Phys. Rev. **124**, 1866 (1961).
[23] B. Lounis and C. Cohen-Tannoudji, J. Phys. II **2**, 579 (1992).
[24] C. Genes, D. Vitali, P. Tombesi, S. Gigan, and M. Aspelmeyer, Phys. Rev. A **77**, 033804 (2008).
[25] S. Barzanjeh, M. Abdi, G. J. Milburn, P. Tombesi, and D. Vitali, Phys. Rev. Lett. **109**, 130503 (2012).
[26] T. Bagci *et al.*, Nature (London) **507**, 81 (2014).
[27] A. T. Reed *et al.*, Nat. Phys. **13**, 1163 (2017).
[28] C. F. Ockeloen-Korppi *et al.*, arXiv:1711.01640; M. J. Woolley and A. A. Clerk, Phys. Rev. A **89**, 063805 (2014); J. Li, I. Moaddel Haghighi, N. Malossi, S. Zippilli, and D. Vitali, New J. Phys. **17**, 103037 (2015); J. Li, G. Li, S. Zippilli, D. Vitali, and T. Zhang, Phys. Rev. A **95**, 043819 (2017).
[29] K. Zhang, F. Bariani, and P. Meystre, Phys. Rev. Lett. **112**, 150602 (2014).
[30] J. Klaers, S. Faelt, A. Imamoglu, and E. Togan, Phys. Rev. X **7**, 031044 (2017).